AD-A161 067 MEASUREMENT OF COMPRESSIONAL WAVE PARAMETERS IN SATURATED SANDS(U) TEXAS UNIV AT AUSTIN APPLIED RESEARCH LABS R D COSTLEY ET AL. 08 MAY 85 1/1

UNCLASSIFIED ARL-TR-85-13 N00014-83-K-0696 F/G 8/13 NL

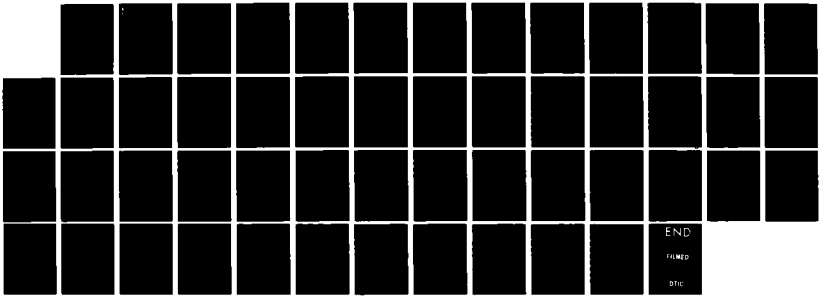

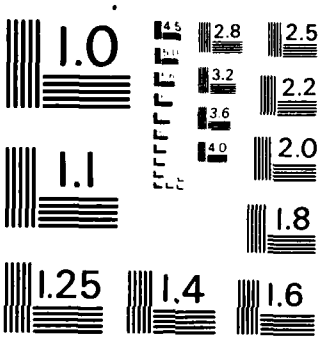

ARL-TR-85-13

Copy No. 23

MEASUREMENT OF COMPRESSIONAL WAVE PARAMETERS IN SATURATED SANDS

R. Daniel Costley, Jr.
A. Marc Bedford
Paul J. Vidmar

APPLIED RESEARCH LABORATORIES
THE UNIVERSITY OF TEXAS AT AUSTIN
POST OFFICE BOX 8029, AUSTIN, TEXAS 78713-8029

8 May 1985

Final Report

1 September 1983 – 31 August 1984

Prepared for:

OFFICE OF NAVAL RESEARCH
DEPARTMENT OF THE NAVY
ARLINGTON, VA 22217

UNCLASSIFIED

SECURITY CLASSIFICATION OF THIS PAGE (When Data Entered)

REPORT DOCUMENTATION PAGE		READ INSTRUCTIONS BEFORE COMPLETING FORM
1. REPORT NUMBER	2. GOVT ACCESSION NO. AD-A161067	3. RECIPIENT'S CATALOG NUMBER
4. TITLE (and Subtitle) MEASUREMENT OF COMPRESSIONAL WAVE PARAMETERS IN SATURATED SANDS		5. TYPE OF REPORT & PERIOD COVERED final report 1 Sep 83 - 31 Aug 84
		6. PERFORMING ORG. REPORT NUMBER ARL-TR-85-13
7. AUTHOR(s) R. Daniel Costley, Jr. A. Marc Bedford Paul J. Vidmar		8. CONTRACT OR GRANT NUMBER(s) N00014-83-K-0696
9. PERFORMING ORGANIZATION NAME AND ADDRESS Applied Research Laboratories The University of Texas at Austin Austin, Texas 78713-8029		10. PROGRAM ELEMENT, PROJECT, TASK AREA & WORK UNIT NUMBERS
11. CONTROLLING OFFICE NAME AND ADDRESS Office of Naval Research Department of the Navy Arlington, Virginia 22217		12. REPORT DATE 8 May 1985
		13. NUMBER OF PAGES 47
14. MONITORING AGENCY NAME & ADDRESS(if different from Controlling Office)		15. SECURITY CLASS. (of this report) UNCLASSIFIED
		15a. DECLASSIFICATION/DOWNGRADING SCHEDULE

16. DISTRIBUTION STATEMENT (of this Report)

Approved for public release; distribution unlimited.

17. DISTRIBUTION STATEMENT (of the abstract entered in Block 20, if different from Report)

18. SUPPLEMENTARY NOTES

19. KEY WORDS (Continue on reverse side if necessary and identify by block number)

compressional velocity
compressional attenuation
Biot theory
viscosity dependence
experiment
sand

20 ABSTRACT (Continue on reverse side if necessary and identify by block number)

This report summarizes research carried out at Applied Research Laboratories, The University of Texas at Austin, during the period 1 September 1983 - 31 August 1984 under Contract N00014-83-K-0696. The focus of this research was to improve the accuracy of velocity and attenuation measurements so that a definitive test of the Biot-Stoll theory could be made. The major accomplishments during this period were refining the design of transducers, improving the procedures for making accurate laboratory measurements of the velocity and

DD FORM 1 JAN 73 1473 EDITION OF 1 NOV 65 IS OBSOLETE

UNCLASSIFIED

SECURITY CLASSIFICATION OF THIS PAGE(When Data Entered)

20. (cont'd)

attenuation of shear and compressional waves in saturated sands, and locating the sources of experimental error. Preliminary measurements of compressional wave parameters were also made as the first step in testing the Biot-Stoll theory.

TABLE OF CONTENTS

LIST OF FIGURES

LIST OF SYMBOLS

R - Rayleigh distance

ω - Angular frequency

f - Frequency

c - Phase velocity

r - Transducer separation

E - Voltage amplitude

E_r - Reference amplitude, amplitude at the smallest separation

λ - Wavelength

K, K_1, K_2, etc. - Arbitrary constants

I. INTRODUCTION

Sonic and ultrasonic techniques are available for determining the acoustic properties of materials by making direct laboratory measurements of the phase velocity and attenuation of harmonic waves. Numerous authors have reported such measurements on saturated sediments. Applied Research Laboratories, The University of Texas at Austin (ARL:UT), has carried out many measurements of this type and has pioneered the development of transducers for the generation and sensing of shear waves.[1-4]

There is currently controversy over the frequency dependence of the shear and compressional attenuations (and hence, on the basis of causality[5] arguments, their velocities) of saturated marine sediments. This frequency dependence is an important basic property of sand sediments that could be related to the unexplained frequency dependence of low frequency propagation in shallow water.[6] Hamilton,[7] using a viscoelastic framework, carried out an extensive examination of reported attenuation values for compressional waves in marine sediments and concluded that these values were consistent with a linear dependence on frequency. Extensive analytical predictions of the phase velocity and attenuation of acoustic waves in saturated sediments have been presented by Stoll and Bryan[8] and by Stoll,[9-11] who based their work on the classical mixture theory of Biot.[12,13] The theory of Stoll and Bryan was further refined by Hovem and Ingram,[4] and by Bedford, Costley, and Stern.[14] These theories, based on the microstructure of the sediment, predict a more complicated frequency dependence than that suggested by Hamilton. In the absence of direct measurements at low frequencies, experiments that test the validity of the Biot approach are needed to determine the correct method to use in extrapolating measurements at higher frequencies to lower frequencies.

ARL:UT recently introduced[15] an important innovation in the study of acoustic properties of saturated sediments. A mixture of water and glycerine was used as the saturating fluid; by varying the ratio of

glycerine to water, the viscosity, density, and bulk modulus of the saturant could be varied in a controlled manner. Since these parameters appear explicitly in the Biot-Stoll equations, this procedure permits a definitive test of the theory. Furthermore, these measurements can be used in a more complete theoretical analysis of the coefficients in the equations. Preliminary measurements[16] indicated that the Biot-Stoll predictions for the dependence on viscosity may not be correct. However, due to large experimental uncertainty, no definitive conclusions could be drawn.

This report summarizes further laboratory measurements at ARL:UT during the period 1 September 1983 - 31 August 1984. The focus of this research was to improve the accuracy of velocity and attenuation measurements so that a definitive test of the Biot-Stoll theory could be made. The major accomplishments during this period were refining the design of transducers, improving the procedures for making accurate laboratory measurements of the velocity and attenuation of shear and compressional waves in saturated sands, and locating the sources of experimental error. Preliminary measurements of compressional wave parameters were also made as the first step in testing the Biot-Stoll theory. This work was carried out by D. Costley under the direction of Dr. A. Bedford, Department of Aerospace Engineering and Engineering Mechanics, The University of Texas at Austin, and Dr. Paul Vidmar, Applied Research Laboratories, The University of Texas at Austin. This work has been submitted by Mr. Costley as part of a Master's thesis in Aerospace and Engineering Mechanics at The University of Texas at Austin.

The remainder of this report is organized as follows. Section II reviews the measurement procedure and preliminary results (forming part of Mr. Costley's Master's thesis). Section III discusses the progress made and suggests directions for future research.

II. EXPERIMENTAL PROCEDURE AND PRELIMINARY RESULTS

A. General Procedure

The objective of this experiment is to determine the phase velocity and attenuation of harmonic compressional waves in a fluid saturated sediment as a function of viscosity of the pore fluid. These results will be compared with those predicted by the Biot-Stoll theory. Since the parameters viscosity, bulk modulus, and density appear in the Biot-Stoll expression for the wave number, these measurements are expected to be a critical test of the theory.

The main focus of the work described here has been to improve the techniques developed by previous investigators[16,17] for measuring the attenuation and phase velocity of compressional waves and to locate the causes of experimental error. The most significant development over earlier work was the redesign of the compressional wave transducers. With this improvement, spherical spreading was established and measured, thus reducing the error caused by the directivity of the transducers. Two identical transducers were built, one serving as a transmitter and the other as a receiver. The transmitter converts an electrical signal, which is generated in an oscillator, into an acoustic signal, which propagates through the sediment. The receiver detects this acoustic signal and reconverts it into an electrical signal which is displayed on an oscilloscope.

The central idea in our measurement procedure is to compare the time delay and amplitude of the output voltage signal at one transducer separation with the same measurements at other separations. From the time delay measurements at different separations, the phase velocity is determined. Similarly, by comparing the different amplitude measurements, the attenuation can be calculated. It is assumed that the coupling between the transducer and the sediment is the same at each separation. This assumption allows us to relate the decay in amplitude only to the increase in transducer separation.

Initially, the transducers are placed approximately 20 cm apart. The time delay from the beginning of the triggered pulse to the fourth positive peak of the received signal is then recorded along with the peak-to-peak amplitude of the fourth cycle of the received signal. The fourth cycle is used so that the measurements are made as close to the steady state part of the signal as possible. The signal is then monitored for at least four hours to ensure that there are no variations in signal amplitude due to changes in the coupling between the sediment and the transducers or due to any settling of the sediment. Four to six readings are taken over this period, and the slight variations about the stabilized value are averaged. The receiver is then moved 2.0 cm closer to the transmitter and the amplitude and time delay measurements are repeated. These measurements are repeated at 2.0 cm intervals until the separation between the transducers is approximately 6.0 cm. Using this set of measurements, the phase velocity and attenuation are determined by finding the least squares fit to the data.

The viscosity of the fluid is then increased by adding glycerine to the mixture. The entire set of measurements is repeated and the phase velocity and attenuation are determined for a new value of viscosity. This procedure is repeated several times, each time with a new value of viscosity. In this way, plots of phase velocity and attenuation versus viscosity can be made and then compared with predictions of the theory.

B. Instrumentation

A schematic of the laboratory equipment is shown in Fig. 1. A continuous tone of 105.0 kHz and 10.0 V peak-to-peak amplitude is generated in the oscillator. The output is sent to a frequency counter, a tone burst generator, and an oscilloscope. The tone burst generator passes a four-cycle pulse of 105.0 kHz to the transmitting transducer. The signal is then cut off for several milliseconds so that the reflections of the signal off the sides of the container and the sediment-water interface will die down before a new four-cycle pulse is sent to the transmitter. Any reflections not suppressed will interfere

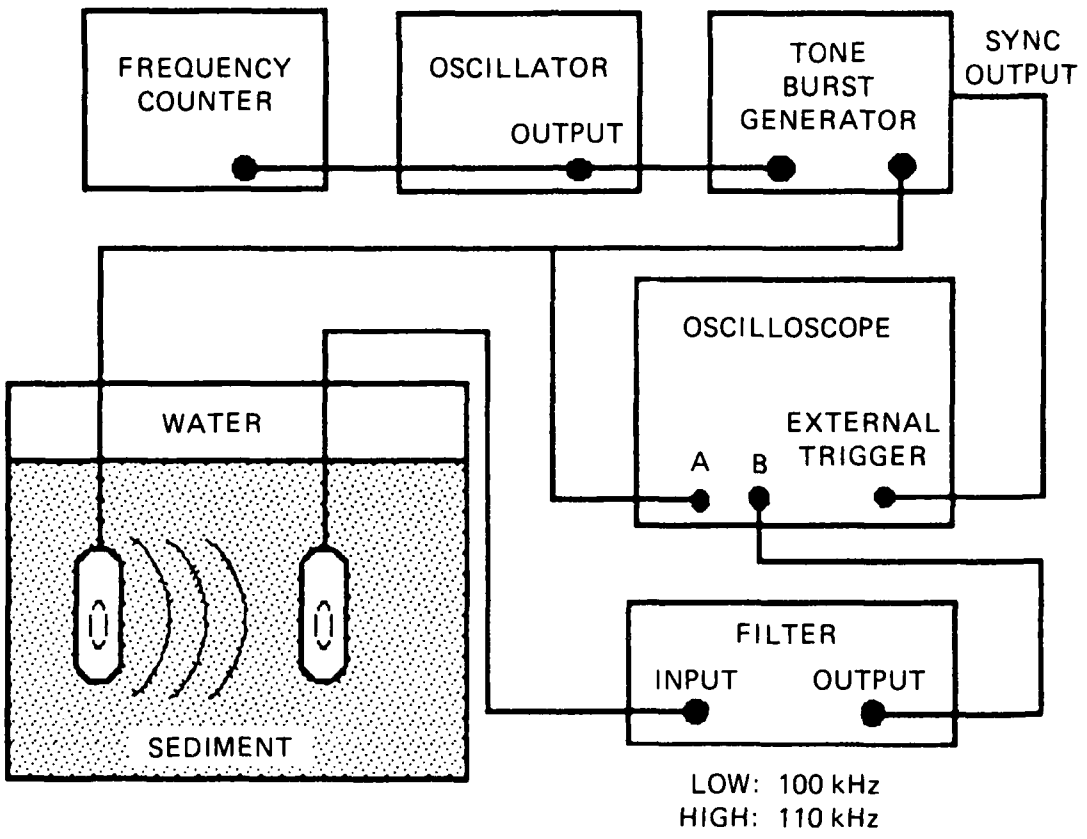

FIGURE 1
SCHEMATIC DIAGRAM OF EXPERIMENTAL EQUIPMENT

ARL:UT
AS-85-54
RDC - GA
1 - 23 - 85

with the signal that follows the direct path between the transducers, and thus produce an error in the signal amplitude and time delay measurements.

The pulse is also displayed on an oscilloscope. The tone burst generator has a synchronized output, which is connected to the external trigger input of the oscilloscope. This causes the oscilloscope trace to trigger at the beginning of the four-cycle pulse.

The acoustic pulse generated in the sediment is detected by the receiving transducer. The transducer converts the acoustic signal into a voltage which is sent through a bandpass filter, and then displayed on the oscilloscope. The low and high cutoff frequencies of the bandpass filter are 100 kHz and 110 kHz, respectively. The filter is used to remove the extraneous frequencies, introduced because the transmitted pulse is the product of a pure tone and the difference of two step functions, from the received signal. The measurements of attenuation and phase velocity will then correspond to the single frequency of 105.0 kHz.

C. Transducers

1. Construction

The two transducers are nearly identical and can be used as either a transmitter or receiver. The transducers were built from a piezoelectric element mounted in a stainless steel plate. A rod was welded onto the plate so that the plate and transducer element could be shoved into the sediment-water mixture. A sketch of a transducer mount is shown in Fig. 2.

The two elements are made of Channelite 5500, manufactured by Channel Industries, Inc. Their thickness and diameter are 3/16 in. and 3/4 in., respectively. Each element has two resonances. In the thickness mode, transducers No. 1 and 2 resonate at 446.4 kHz and

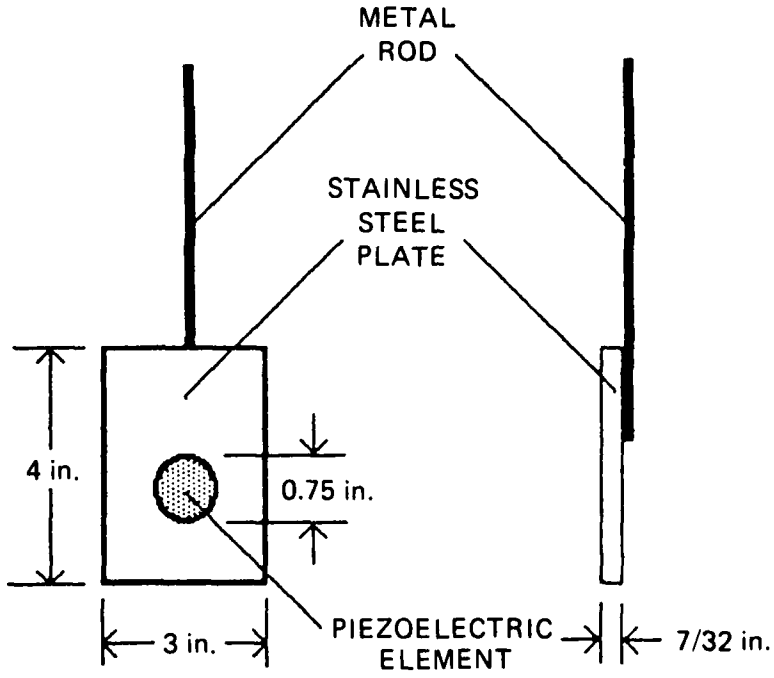

FIGURE 2
DIMENSIONS OF TRANSDUCERS

445.2 kHz, respectively. In the radial mode, transducers No. 1 and 2 resonate at 105.5 kHz and 105.1 kHz, respectively. In this experiment, the transducers are used in the radial mode, at 105.0 kHz.

To build the transducers, a 7/8 in. hole was drilled through the steel plate. The element was mounted in the hole with a layer of corprene placed between it and the steel plate; a layer of corprene was also attached on the backside of the transducer. A wire was soldered on each face of the element, and the two wires were placed in a shielded, waterproofed sheath.

Corprene, which has a much lower acoustical impedance than the piezoelectric element or the sediment-water mixture, is used on the backside of the element as a pressure release material. Thus most of the energy is radiated from the front side of the transducer, toward the receiver, thereby producing a higher signal-to-noise ratio.

The plate and the element were designed to act as a radiating piston in a rigid baffle. In this way, the geometrical spreading and the directivity of the transducer could be calculated and verified by measurement.

The circular radiating surface was large enough to allow a substantial transfer of energy from the piezoelectric element to the sediment. Since this surface area was large compared to the individual sediment grains, problems associated with the coupling of the transducer to the sediment were reduced.

2. Geometrical Spreading

Since the geometrical spreading in the nearfield is very complicated and varies with distance from the source, the transducers were designed for use in the farfield. The Rayleigh distance is roughly the distance away from the source at which the farfield begins. At distances greater than the Rayleigh distance, the amplitude of the

signal decays as 1/r, due to the geometrical spreading of the signal. Here, r is the distance from the source.

The Rayleigh distance for a circular piston in an infinite, rigid baffle is given by[18]

$$R = \frac{ka^2}{2} \quad ,$$

where a is the radius of the piston, $k=\omega/c$ is the wave number, and ω is the angular frequency. Note that R is inversely proportional to the phase velocity c. For these transducers, operating at a frequency of 105.0 kHz, this formula gives a Rayleigh distance of 2.0 cm in water. Spherical spreading is expected at separations of about 4.0 cm or greater.

For a lossless medium in which there is 1/r spreading, the signal amplitude satisfies the following relation.

$$E/E_r = K\lambda/r \quad ,$$

where E is the signal amplitude, E_r is the reference amplitude, λ is the wavelength, and K is a calibration constant. Taking the logarithm of both sides gives

$$\log \frac{E}{E_r} = -\log \frac{r}{\lambda} + \log K \quad .$$

Thus, if the signal amplitude is measured as a function of separation for separations greater than the Rayleigh distance, the points will fall on a straight line with a slope of -1 when plotted on log-log graph paper.

To experimentally verify that there is spherical spreading in water at separations greater than 4.0 cm, the amplitude of the acoustic signal was measured as the range was varied from 4.0 cm to 20.0 cm, in

2.0 cm increments. A least squares fit through the points on a log-log plot of range versus amplitude reveals a slope of m=-0.9914 of the equation

$$\log \frac{E}{E_r} = m \log \frac{r}{\lambda} + \log B \quad .$$

If the point corresponding to r = 4.0 cm is omitted, the slope is m=-1.0061 as shown in Fig. 3. At these distances, it can be assumed that there is no absorption in water and the total losses can be attributed to geometrical spreading. Therefore, this test shows that there is spherical spreading at separations greater than 4.0 cm.

Since the phase velocity is greater in the sediment-water mixture than in water, the Rayleigh distance is even smaller in the mixture. Thus it is known that the geometrical spreading in the sediment is spherical at separations greater than 4 cm.

3. Directivity

Since the transducers are directional, great care has to be taken in moving the receiving transducer to keep the transducers on each other's axes where the signal amplitude is maximum. The axis is the imaginary line running through the center of the circular element and perpendicular to its face. The alignment problem is lessened if the radiation pattern of the transducer is sufficiently wide that slight errors in realigning the receiver exactly on the axis of the transmitter will cause only a slight error in the on-axis signal amplitude.

By treating the transducer as a circular piston in an infinite, rigid baffle, the half-power angle can be calculated. If p(0,r,t) is the on-axis pressure, then the half-power angle is the angle at which the pressure is given by[18]

$$p(\theta_{HP},r,t) = \frac{1}{\sqrt{2}}\, p(0,r,t) \quad .$$

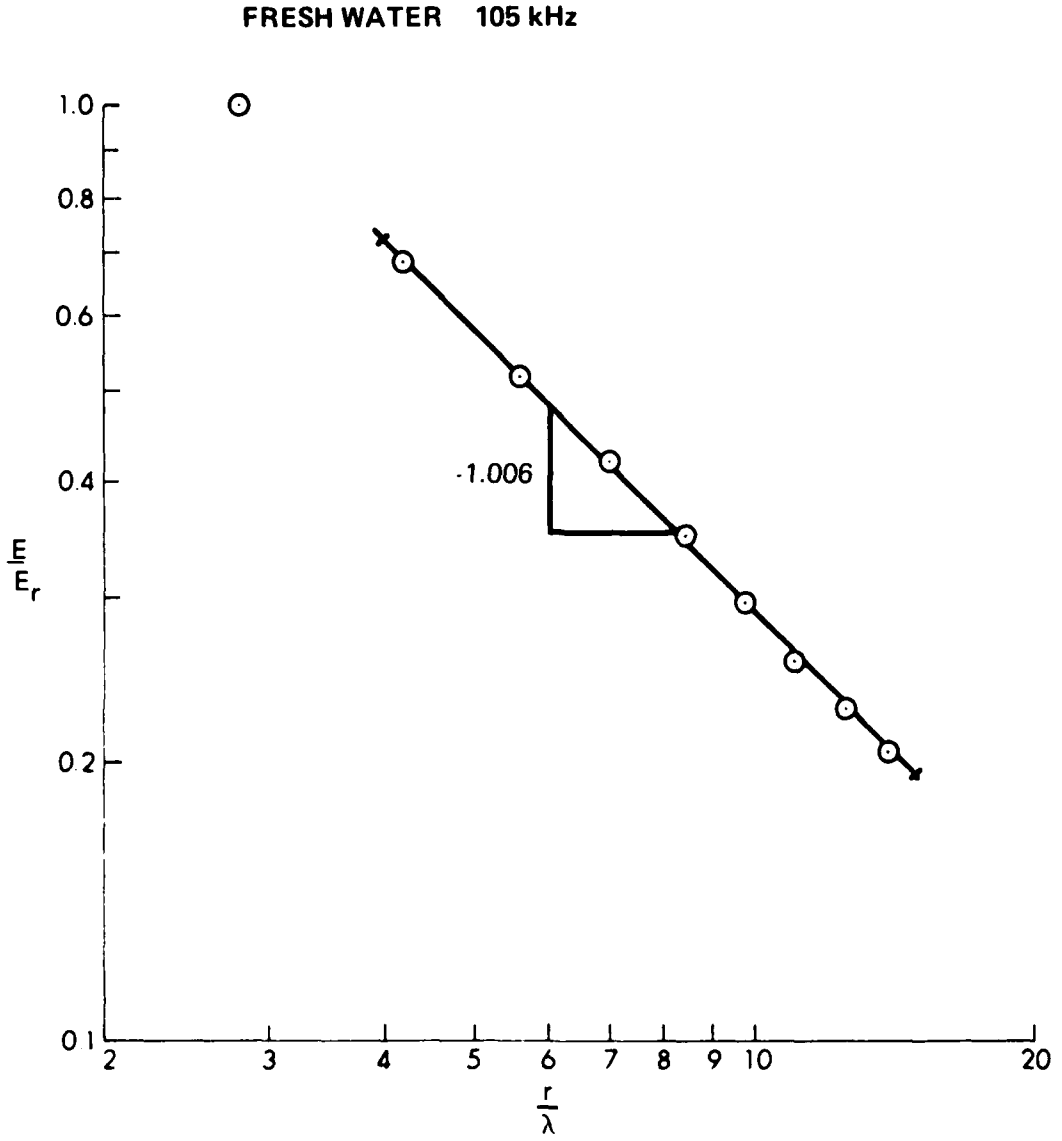

$$\log \frac{E}{E_r} = -\log \frac{r}{\lambda} + \log K$$

$$E = \frac{\lambda K E_r}{r} = \frac{K'}{r}$$

FIGURE 3
SPHERICAL SPREADING IN FRESH WATER

ARL:UT
AS-84-1035
DRC-GA
11-19-84

For a circular piston, the half-power angle is[18]

$$\sin\theta_{HP} = 1.616/(ka) \quad .$$

In fresh water, at a frequency of 105.0 kHz, the calculated half-power angle for these transducers is 22.6^{o}.

Figures 4 and 5 show the measured directivity of the two transducers in fresh water. Again, it is seen that the model of the transducer as a circular piston on a rigid baffle works well. The directivity patterns for both transducers show that the half-power angle, the angle at which the pressure is 3.0 dB below the on-axis pressure, is about 20^{o}.

Since transducer No. 1 is used as the receiver in this experiment, and is the one being moved after each reading, it is desired that the response of this transducer especially be constant for small angles off axis. This is so that failure to exactly realign the transducers will still give a reliable measurement of the on-axis value of the signal amplitude. Figure 4 shows that the sound pressure level for transducer No. 1 varies less than 0.5 dB for 7.0^{o} on either side of the axis. A 0.5 dB difference in sound pressure level implies that the actual pressure varies less than 6.0% from the on-axis value. Actually, the SPL for transducer No. 1 is essentially constant for angles up to 3.0^{o} off axis.

For mediums such as saturated sediments, in which the sound speed is higher than that of water, the half-power angle would be even greater. A typical compressional wave speed for a sediment-water mixture is 1800 m/s.[17] At the same frequency that is being considered (105.0 kHz), this means a half-power angle of 28^{o}. Thus, for small angles off axis, the signal amplitude would vary even less from the on-axis value in the mixture than it would in water. In the measurements taken in this experiment, care was taken to position the receiver in the

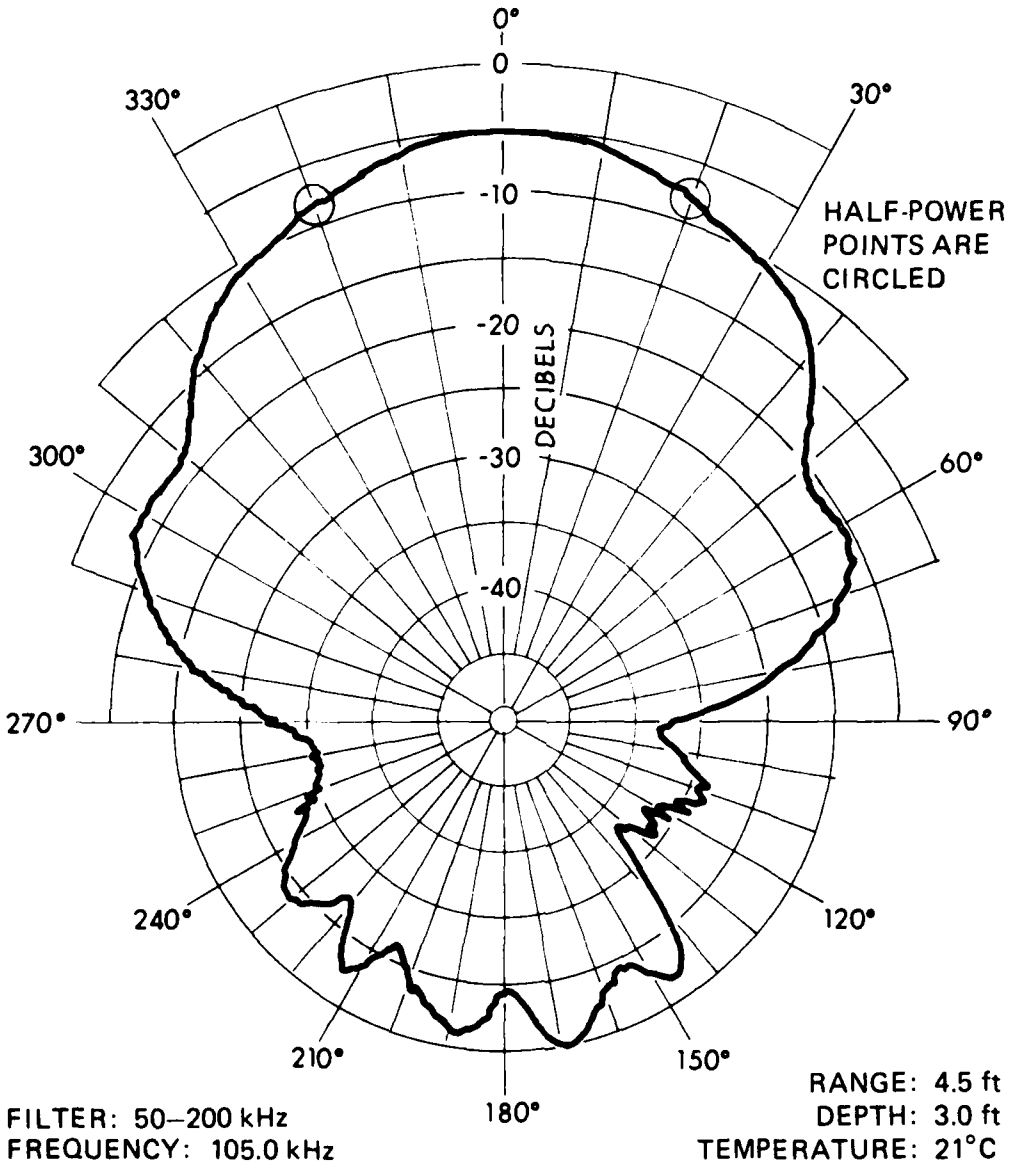

FIGURE 4
DIRECTIVITY PATTERN IN HORIZONTAL PLANE
FOR TRANSDUCER No. 1 IN FRESH WATER

ARL:UT
AS-85-56
RDC - GA
1 - 23 - 85

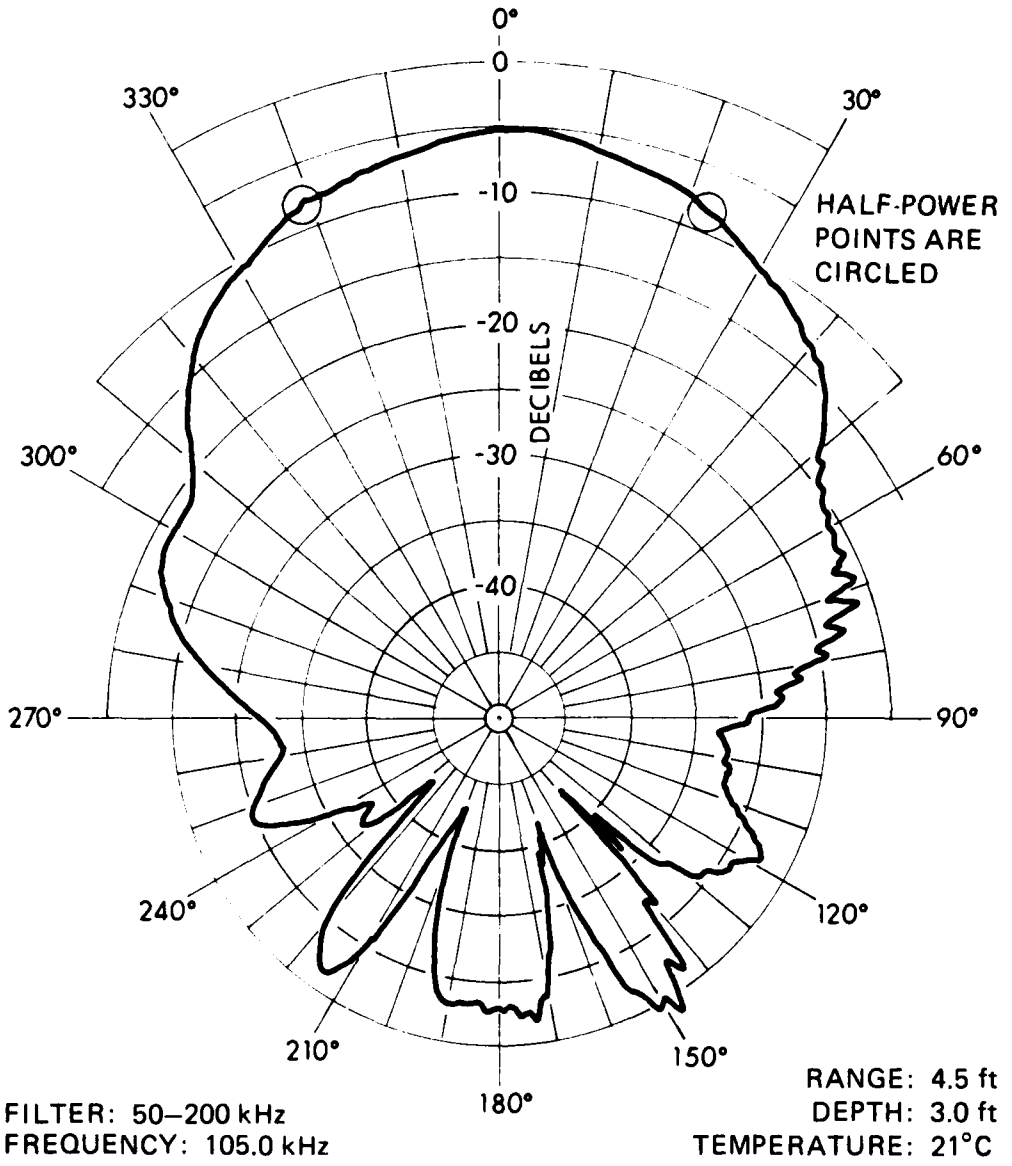

FIGURE 5
DIRECTIVITY PATTERN IN HORIZONTAL PLANE
FOR TRANSDUCER No. 2 IN FRESH WATER

sediment with no more than 4^{o} variation in the angle off axis. Thus, we have confidence that the on-axis signal amplitudes were measured accurately.

D. Sediment Preparation

The sediment is made up of MS-MH size glass beads manufactured by Ferro Corporation, Jackson, Mississippi. The grain size distribution is shown in Fig. 6.[17]

The sediment-water mixture was prepared in a 5 gal plastic bucket in the following manner. The bucket is approximately 35 cm high and 29 cm in diameter. The liquid in the sediment-water mixture is circulated by a Masterflex tubing pump. Before the mixture was put in the bucket, the outflow tube was attached to the bottom of the bucket with duct tape. The bucket was then partially filled with de-ionized water and the input hose was put in the water. The pump was turned on so that all of the air was driven from the tube. A capful of BIO-CLEAN III algaecide was added to the water to retard the growth of micro-organisms.

The glass shot was then poured slowly into the water until the sediment-water mixture was 24 cm deep. Pouring was halted at intervals and the mixture kneaded like bread dough to remove air trapped in the beads. A layer of water, approximately 6 cm thick, was left on top of the sediment mixture and the pump input hose was suspended in the layer, as shown in Fig. 7.

To remove any air remaining in the mixture, the mixture was vibrated in excess of 6 hours. The mixture was left undisturbed overnight. The next day, the transducers were shoved into the mixture so that the centers of the elements were 12 cm into the sediment.

To increase the glycerine concentration of the liquid, glycerine was poured into the liquid on top of the mixture and the pump was turned

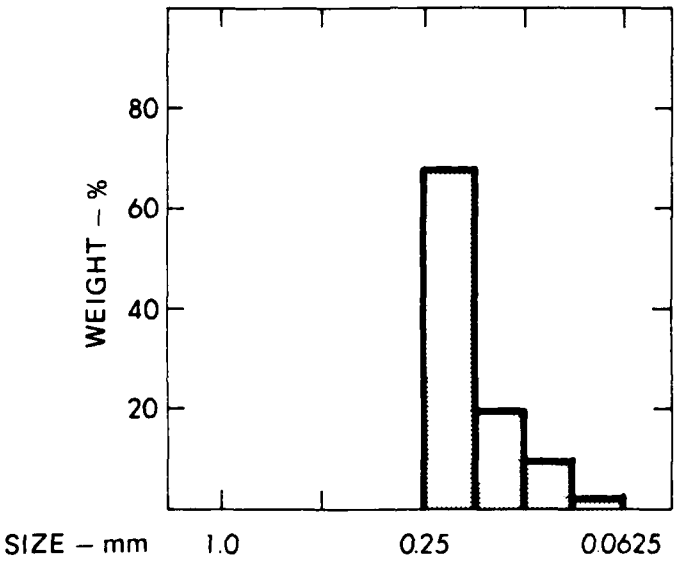

FIGURE 6
GRAIN SIZE DISTRIBUTION FOR MS-MH SIZE BEADS

ARL:UT
AS-85-58
RDC - GA
1 - 23 - 85

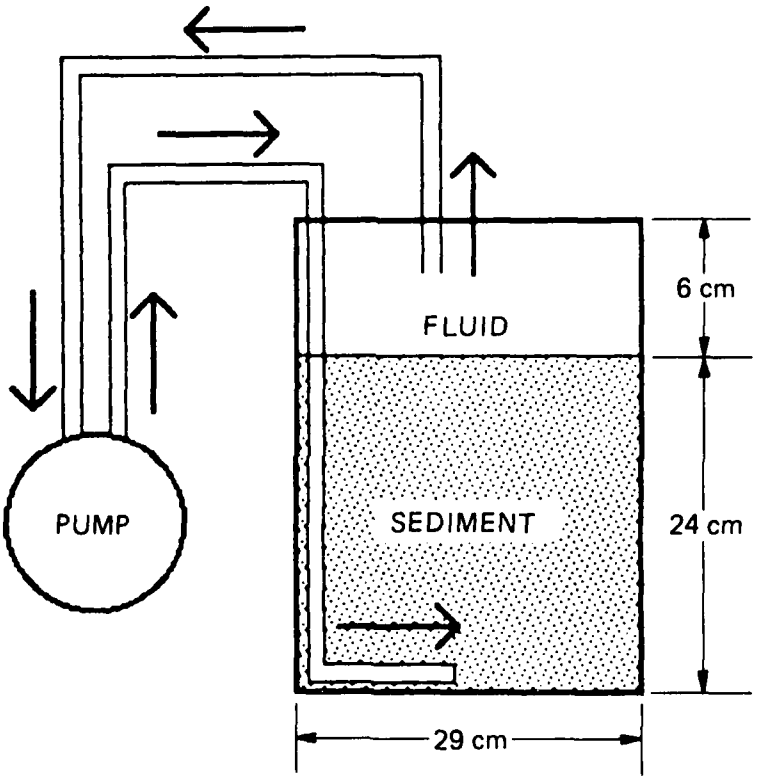

FIGURE 7
CIRCULATING THE PORE FLUID

ARL:UT
AS-85-59
RDC - GA
1 - 23 - 85

on and run until the liquid in the bucket was well mixed. A capful of algaecide was added while the liquid was being circulated to further retard the growth of micro-organisms. The specific gravity of the liquid was measured several times while the liquid was being circulated. The liquid was considered well mixed after the values of specific gravity had stabilized. This usually occurred after about 3 hours. The specific gravity was measured using a hydrometer and the value of viscosity was read from a table containing the values of viscosity for varying concentrations of glycerine-water solutions.[19]

E. Measurements and Preliminary Results

1. Phase Velocity

The oscilloscope trace was triggered at the beginning of the transmitted four-cycle pulse. The arrival time to the fourth positive peak on the received signal was measured with a digital readout on the oscilloscope. This was first done at a transducer separation of approximately 20 cm and then at 2.0 cm increments down to a separation of 6 cm.

If these arrival times were then plotted on a time versus distance graph, with time as the horizontal axis, the points should fall on a straight line parallel to the characteristic of the wavelet. The slope of this line is the phase velocity. Therefore, to find the phase velocity a least squares routine is used to fit the best straight line through these points. Since the line is parallel to a characteristic, the equation of the line is of the form

$$r = ct + B \quad ,$$

where c is the phase velocity and B is the intercept of the r axis. If the time were measured from the fourth positive peak on the transmitted pulse to the same peak on the received pulse, B would ideally be zero (for a nondispersive medium) and the least squares line would be the

same as the characteristic. But since time is measured from the beginning of the triggered pulse, and since there are additional time delays associated with the circuitry and transducers, B turns out to be negative.

This method was tested using two different size beads with fresh water as the pore fluid: the MS-MH size, which was used in the experiment, and the MS-L size beads, which are a smaller size. The results of these preliminary tests are shown in Figs. 8 and 9. The linear correlation coefficient is a number between 0 and 1 that gives an indication of how well the data points fit a straight line. A coefficient of 1 represents perfect linear correlation and a coefficient of 0 represents no correlation. It can be seen in both of these figures that the correlation between the data and the straight line is very good. The good correlation indicates that the disturbances in the sediment, caused by moving the transducer to each separation, has a negligible effect on the measurements.

In order to check the validity of our procedure, we measured the phase velocity in water at room temperature, approximately 25°C, six times. Each of these results was between 1492 m/s and 1508 m/s. The average of these measurements was 1501 m/s. By linear interpolation of tabulated values of sound speed as a function of temperature, we found that the speed of sound at 25°C in fresh water is 1496 m/s. The average then has an error of only 0.33% while the extreme values have errors of -0.3% and 0.8%.

In another check, we compared our results to results obtained by Bell,[17] Shirley,[16] and Hovem and Ingram.[4] We measured the phase velocity three separate times in MS-MH beads with fresh water as the pore fluid. The three results are shown in Table I, along with the other results mentioned. Comparison with these other results indicates that our results are valid. But the comparison also suggests that the velocity is strongly dependent on the depth of the transducers in the sediment.

BEAD TYPE: MS-MH
FREQUENCY: 105 kHz VISCOSITY: 0.893 cP

TIME – μs	SEPARATION – cm
65.88	5.65
77.63	7.65
88.98	9.65
100.12	11.65
112.07	13.65
121.38	15.65
133.23	17.65
142.31	19.65

VELOCITY: 1820 m/s
STANDARD DEVIATION OF VELOCITY: 24 m/s
LINEAR CORRELATION COEFFICIENT: 0.9995

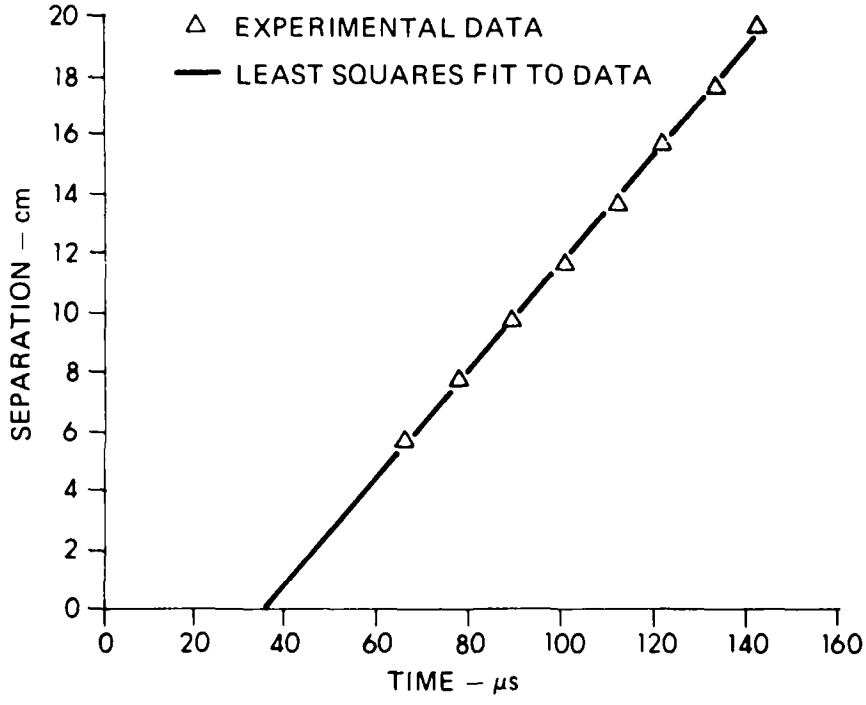

FIGURE 8
PHASE VELOCITY IN MS-MH BEADS

ARL:UT
AS-85-60
RDC - GA
1 - 23 - 85

BEAD TYPE: MS-L
FREQUENCY: 105.0 kHz VISCOSITY: 0.893 cP

TIME – μs	SEPARATION – cm
63.62	5.65
73.39	7.65
83.49	9.65
95.51	11.65
107.15	13.65
118.60	15.65
131.73	17.65
138.98	19.65

VELOCITY: 1791 m/s
STANDARD DEVIATION OF VELOCITY: 34 m/s
LINEAR CORRELATION COEFFICIENT: 0.9989

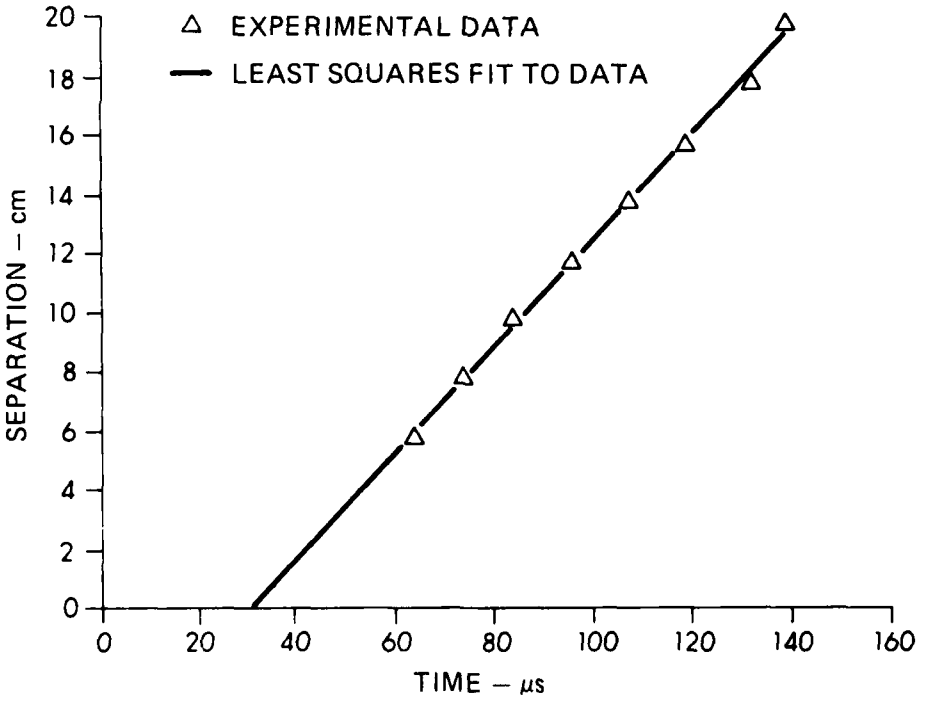

FIGURE 9
PHASE VELOCITY IN MS-L BEADS

TABLE I

COMPARISON OF VELOCITY RESULTS IN MS-MH AND MS-L SIZE BEADS

	Frequency (kHz)	Depth (cm)	Velocity (m/s)	
			MS-MH	MS-L
Bell	120.0	9	1809	1854
Shirley	114.0	10	1808	
Hovem & Ingram	100.0	20	1922	
Present Study	105.0	12	1820	1791
	105.0	12	1840	
	105.0	12	1866	

The comparison in the MS-L size beads is not nearly so good. Our first trial measurement in sediments was made in the MS-L size beads. Since the standard deviation accompanying this measurement is so large (34 m/s) and since in all subsequent measurements the standard deviation was substantially reduced, the discrepancy is attributed to experimental error and carelessness in precisely determining the separation. As the experiment progressed, the technique improved and the error decreased.

Obviously, sound speed measurements in sediments are not nearly as repeatable as measurements made in water. One reason for this is the uncertainty in the separation measurement. In the sediment, this uncertainty is estimated to be 0.1 cm. At a separation of 20 cm, this represents a relative uncertainty of 0.5%, while at 6 cm the uncertainty is 1.7%. The uncertainty in the time delay measurement is negligible compared to this. Relative uncertainties of 0.5% and 1.7% in the separation represent absolute uncertainties in the velocity of 10 m/s and 30 m/s, respectively. The standard deviations shown in Figs. 8 and 9 were derived from the least squares method. The assumptions made in these calculations were that the absolute uncertainties in the vertical axis, or separations, are equal, and the uncertainties in the horizontal axis are negligible. Both of these assumptions are appropriate, and the standard deviations calculated from this method are consistent with uncertainties in separation and hence are a realistic measure of the uncertainty in the velocity.

The standard deviations of the velocities were less than 15 m/s after the first trial measurements. This indicates that as the experiment progressed, the technique improved and the uncertainty decreased.

2. Attenuation

In the sediment, the losses are due to both geometrical spreading and absorption of the medium. Therefore, to calculate the attenuation in the medium, the geometrical spreading must be taken into

account. As discussed in Section II.C.2, the transducers were designed so that the Rayleigh distance would be relatively small compared to the sediment sample. At distances greater than the Rayleigh distance, the signal amplitude decays as 1/r due to the spherical spreading, where r is the separation between the transducers. This distance was calculated for both water and sediment. The calculation for water was then verified by acoustic measurements. These measurements show that the geometrical spreading in the sediment was indeed spherical at the distances at which the attenuation measurements were taken. Using the spherical spreading, the losses due to absorption in the sediment can be readily determined. A detailed discussion of this procedure follows.

The measurements establishing the 1/r decay of the signal amplitude due to geometrical spreading has been discussed in Section II.C.2. The absorption due to the medium can be determined by measuring the amplitude of the signal and assuming that the amplitude varies as

$$E = \frac{K}{r} e^{-\alpha r} \quad . \tag{1}$$

Here, K is a calibration constant with units of volts × length and α is the attenuation in nepers per unit length. The 1/r factor in Eq. (1) takes into account the spherical spreading and the exponential term takes into account the absorption of the medium. It is also assumed that the coupling between the sediment and the transducer is the same at each separation. Thus, the decay in the amplitude of the signal is attributed only to the increase in separation.

The attenuation is determined by comparing the amplitudes measured at various separations. To do this, one of the amplitude measurements and the separation at which it is measured are designated as reference values E_r and r_r, respectively. In this experiment, r_r is the smallest separation at which measurements are taken and $E_r=E$ at $r=r_r$.

Therefore, the following relation holds.

$$E_r = \frac{K}{r_r} e^{-\alpha r_r} \quad .$$

From this and Eq. (1) it follows that:

$$\alpha (r-r_r) = \ell n \left(\frac{E_r r_r}{Er} \right) . \qquad (2)$$

Therefore, if $\ell n \left[(E_r r_r)/Er \right]$ versus $(r-r_r)$ is plotted, the points should fall on a straight line and the slope of the line would be the attenuation. To find the slope of this line, and thereby the attenuation, the method of least squares is used.

This technique was tested using two different size beads with fresh water as the pore fluid: the MS-MH size, which was used in the experiment, and the MS-L size, which are smaller beads. The results of these preliminary tests are shown in Figs. 10 and 11. As in the phase velocity case, a linear correlation coefficient of near 1 indicates a very close correlation between the data and the straight line.

The standard deviation can be calculated for this method, assuming that the uncertainties in all of the data points are equal and that there is no error in the values along the horizontal axis. Because these assumptions are false, the standard deviation calculated from the least squares method is too low. But the attenuation can be calculated by other means, and from these calculations a realistic estimate of the error can be made.

A physical interpretation of the sources of error can be acquired by calculating the attenuation directly, using Eq. (2) with the data at any two separations. If the data for MS-MH beads corresponding to separations of 5.65 cm and 19.65 cm are used, as shown in Fig. 11, the attenuation turns out to be 2.28 Np/m. We can calculate a Pythagorean estimate of the uncertainty in the attenuation by using the relation[20]

BEAD TYPE: MS-L
FREQUENCY: 105.0 kHz VISCOSITY: 0.893 cP

AMPLITUDE – V	SEPARATION – cm
0.2800	5.65
0.1970	7.65
0.1430	9.65
0.1060	11.65
0.0820	13.65
0.0652	15.65
0.0516	17.65
0.0430	19.65

ATTENUATION: 4.71 Np/m
STANDARD DEVIATION OF ATTENUATION: 0.14 Np/m
LINEAR CORRELATION COEFFICIENT: 0.9974

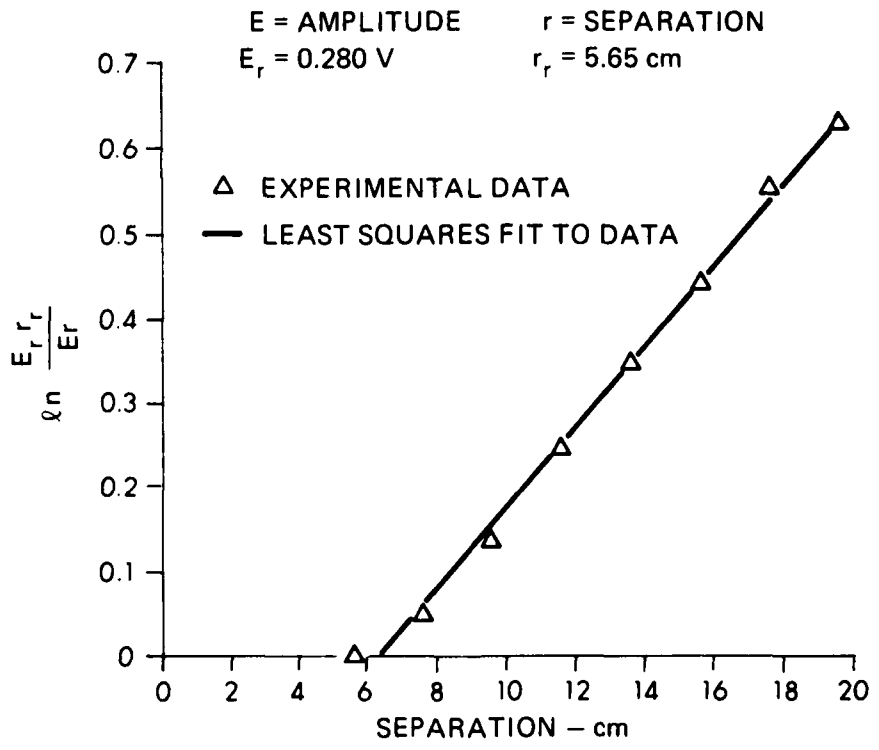

FIGURE 10
ATTENUATION IN MS-L BEADS

BEAD TYPE: MS-MH
FREQUENCY: 105.0 kHz VISCOSITY: 0.893 cP

AMPLITUDE – V	SEPARATION – cm
0.3720	5.65
0.2690	7.65
0.2004	9.65
0.1570	11.65
0.1300	13.65
0.1074	15.65
0.0892	17.65
0.0777	19.65

ATTENUATION: 2.40 Np/m
STANDARD DEVIATION OF ATTENUATION: 0.09 Np/m
LINEAR CORRELATION COEFFICIENT: 0.9962

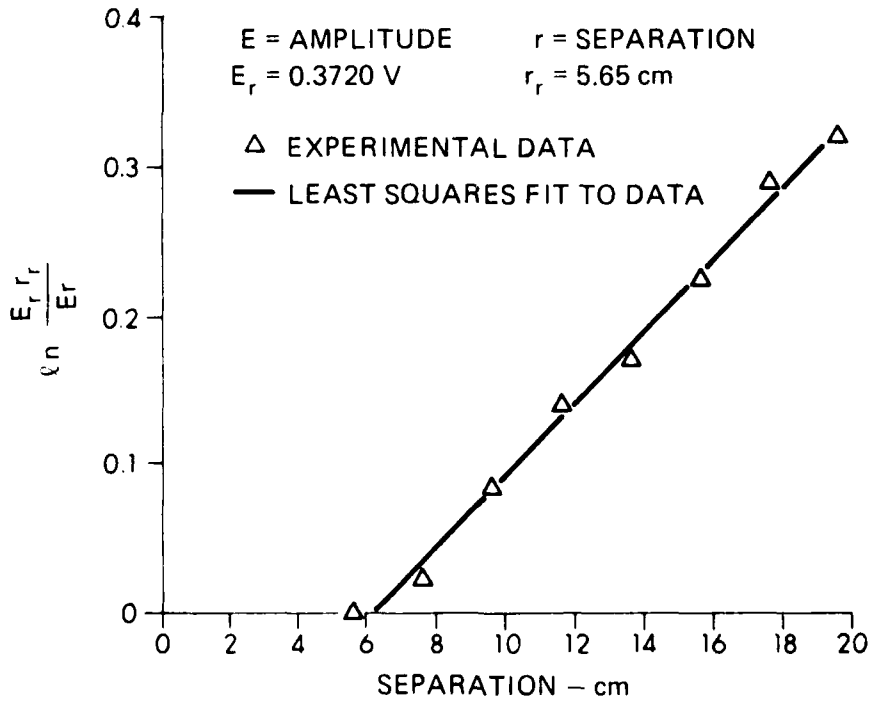

FIGURE 11
ATTENUATION IN MS-MH BEADS

$$\sigma_i^2(r-r_r)^2 = \sigma_r^2(\alpha^2 + \alpha^2\,\alpha/r + 1/r^2)_{ref} + \sigma_r^2(\alpha^2 + 2\alpha/r + 1/r^2) \quad , \quad (3)$$

$$+ (\sigma_E/E)^2_{ref} + (\sigma_E/E)^2$$

where σ_E and σ_r denote the uncertainties, or standard deviations, in the amplitude and separation, respectively, and where the quantities marked "ref" signify that the separations and amplitudes correspond to the separation of 5.65 cm. To perform this calculation, the uncertainties in the separation and the amplitude, σ_r and σ_E, must first be determined. The uncertainty in the separation is estimated to be 0.1 cm.

The uncertainty in the amplitude has two sources. The first one is instrumental; that is, the oscilloscope can be read accurately to 1/4 of a gradation. Because the scale is changed at different separations, since the amplitude grows with decreasing r, this type of uncertainty increases with decreasing separation.

The second source of uncertainty in E is due to the uncertainty in r. Since the amplitude is a function of r, as was assumed in Eq. (1), any uncertainty in r produces an uncertainty in E. This type of error can be estimated from the relation

$$\sigma_E = \sigma_r \frac{\alpha E}{\alpha r} = \sigma_r E(\alpha r + \frac{1}{r}) \quad .$$

By calculating this uncertainty and comparing the results with the instrumental uncertainty at each separation, it can be seen that over 80% of the uncertainty in E is due to the uncertainty in r. Using Eq. (3) and the values in the rows in Table II corresponding to r = 19.65 cm and r = 5.65 cm, the uncertainty in the direct calculation is found to be 0.522 Np/m. Note from Eq. (3) that the uncertainty σ_i is inversely proportional to the difference between the two separations being compared. Thus, one way to improve the measurements would be to increase the distances over which the measurements are taken.

TABLE II

ANALYSIS OF ERRORS IN ATTENUATION

r (cm)	E (V)	$\sigma_{E/E}$	$\sigma_r\sqrt{(\alpha^2+2\alpha/r+1/r^2)}$	σ_i (Np/m)	α_i (Np/m)
5.65	0.372	0.0380	0.000404		
7.65	0.269	0.0407	0.000239	3.06	1.057
9.65	0.2004	0.0407	0.000239	1.606	2.082
11.65	0.157	0.0460	0.000121	1.029	2.317
13.65	0.130	0.0478	0.000095	0.813	2.116
15.65	0.1074	0.0533	0.000077	0.613	2.408
19.65	0.0777	0.0587	0.000056	0.522	2.283

$$\sigma_\alpha^2 = \frac{1}{\sum (1/\sigma_1)^2} \quad \text{so that} \quad \sigma_\alpha = 0.296 \text{ Np/m}$$

$$\alpha = \sigma_\alpha^2 \sum (\alpha_i/\sigma_i^2) = 2.266 \text{ Np/m}$$

Using each pair of data shown in Fig. 11, the attenuation can be calculated seven times in this way, and the values designated as α_i. These seven values of attenuation can then be weighted with their corresponding uncertainties σ_i, and averaged as shown in Table II.[20] The resulting average is a better estimate of the attenuation than any of the individual attenuations, and the standard deviation calculated from this method is a better estimate of the uncertainty. Although this value of α differs by 5% from the least squares value, this standard deviation is a more realistic estimate of the uncertainty.

In calculating the attenuation using this method, the error in the reference separation and amplitude is repeated in each of the seven calculations. Thus, if that measurement is particularly bad, the error in it will be compounded in the final result. To avoid this type of error, the attenuation can be calculated with any two pairs of data, E and r. The values corresponding to r = 5.65 cm do not necessarily need to be the reference separation and amplitude. Since there are eight pairs of data, there are 28 unique ways to calculate using Eq. (2). The unweighted mean of these 28 attenuations and the standard deviation of this mean can easily be calculated. For the MS-MH beads of Fig. 11, this mean is α = 2.38 Np/m and the standard deviation is α = 0.47 Np/m. This value of the attenuation differs by only 0.6% from the least squares value. But this standard deviation is larger than the one calculated from the weighted averages. This may signify that the estimate of the uncertainty in r used in that calculation, σ_r = 0.1 cm, was too low. In later calculations, however, there is better agreement between these two calculations of the standard deviation. This suggests that the separation was determined more precisely as the experiment progressed. Another reason for the discrepancy is that all of the attenuations are weighted equally in calculating the mean. But as can be seen from Eq. (3), the uncertainty decreases as the difference between the two separations increases. Thus, the standard deviation calculated by this method represents an upper bound of the actual uncertainty in the attenuation.

The attenuation was calculated for each value of viscosity using the method of least squares and the mean of all combinations. In each case, the two values of attenuation differed by less than 1%. But we feel that the standard deviation associated with the mean of all combinations was more realistic.

It can be noted that the uncertainty in the separation is by far the biggest source of error. Therefore, to improve these measurements, a more accurate method for determining the separation of the transducers would have to be devised. Toward this end, the separations were corrected using the velocity results. The attenuations were then calculated by the mean of all combinations with these corrected separations. These attenuations were within 1% of the attenuations calculated by the other methods, except for the case of the MS-MH beads of Fig. 11 where the difference was 2.5%. In all but a few cases, the standard deviation was substantially reduced. Thus, the attenuation was calculated by the mean of all combinations. In all but those few cases where the standard deviation was not reduced, the separations were corrected using the velocity results. Reducing the data in this way, we are confident that the attenuations were determined within 3 dB/m, except for a few cases.

3. Comparison of Results: Attenuation

To determine the validity of the attenuation results, the measurements in the water saturated beads, with no glycerine added, were compared to the results of David Bell.[17] His attenuation measurements are given in decibels per wavelength. Converting his results to nepers per meter at 105.0 kHz gives the values 5.45 Np/m and 3.13 Np/m for MS-L and MS-MH size beads, respectively.[3]

The discrepancy in attenuation between Bell's values and those presented in Figs. 10 and 11 is 0.74 Np/m for MS-L and 0.73 Np/m for MS-MS. Since this difference is too large to be attributed to experimental error, an effort was made to explain it.

In order to account for the geometrical spreading of the transducers, Bell measured the amplitude decay in water at 120 kHz and the amplitude decay in the sediment at the same frequency. He assumed that the only losses in the water were due to geometrical spreading and that the losses in the sediment were due to geometrical spreading and the attenuation. He then assumed that the losses due to geometrical spreading in the sediment were the same as in the water at that same frequency. Therefore, to calculate the attenuation in the medium he subtracted the spreading losses, which he determined from his measurements in water, from the total losses.[17]

In doing this, he assumed that the geometrical spreading in the water was the same as in the sediment for measurements taken at the same frequency. But the Rayleigh distance, which is a measure of the distance at which spherical spreading starts, is inversely proportional to the sound speed. Since the sound speed is greater in the sediment than in the water, the Rayleigh distance is smaller in the sediment than in the water. Also, the distances at which he took his measurements were less than the Rayleigh distance for his transducers, so that in water his amplitude did not vary as 1/r. Therefore, the losses due to geometrical spreading were less in the water than in the sediment. The extra geometrical spreading that was occurring in the sediment was attributed to absorption in the sediment resulting in a value of attenuation that was too large.

We also compared our measurements in MS-MH beads with those made by Shirley[16] and Hovem and Ingram.[4] These results are summarized in Table III. Shirley's results, like Bell's, are much higher than ours. We believe that he measured the attenuation in the same way that Bell did. Thus his results differ from ours for the same reason that Bell's do.

Hovem and Ingram's[4] results at 100 kHz also differ significantly from ours. If their results at only this one frequency

TABLE III

COMPARISON OF ATTENUATION RESULTS IN MS-MH SIZE BEADS

	Frequency (kHz)	Depth (cm)	Attenuation (dB/m)
Present Study	105.0	12.0	20.85
			20.74
			21.61
Bell	120.0	9.0	27.10
Shirley	114.0	10.0	30.91
Hovem & Ingram	60.0	20.0	24.86
	80.0	20.0	17.63
	100.0	20.0	13.20
	150.0	20.0	19.65

are considered, one might be led to the conclusion that the measured attenuation is very much dependent on the depth of the transducers in the sediment. But if their results at other frequencies in that range are considered, it can be seen that their data exhibit a significant amount of dispersion. It is difficult to say whether this dispersion is due to actual physical processes or to scatter in the data. Other frequency dependent measurements need to be taken to investigate this.

There were also several assumptions made in our measurements which could affect the validity of the attenuation results. One assumption was that the coupling between the transducer and the sediment was the same in each case. Since this is not a trivial assumption, an effort was made to justify it. Each time the transducer was moved, the sediment-water mixture was vibrated gently for approximately 30 minutes. The mixture was then left undisturbed for an additional half hour before another measurement was taken. Four or five more readings were then taken over the next 3-4 hours. Since the voltage and travel time readings never changed over this period of time, except for small variations attributed to experimental uncertainty, it was assumed that the coupling between the transducer and sediment did not vary.

F. Summary

The measurement techniques described in this report are refinements of techniques developed and used previously.[4,16,17] The main effort, thus far, has been to design a valid technique for measuring the phase velocity and attenuation of compressional waves in sediments. The main improvement over the earlier work has resulted from redesigning the compressional wave transducers so that the geometrical spreading and directivity can be predicted. With this improvement, spherical spreading is established at the separations at which these measurements are taken. Thus the losses due to geometrical spreading are accurately accounted for when analyzing the data.

III. DISCUSSION

The purpose of the work presented here has been to design an experiment that will examine the dependence of compressional wave propagation in fluid saturated sands on the viscosity of the pore fluid. Since this dependence is predicted by the Biot-Stoll equations, these measurements should be a critical test of the theory.

Experiments of this type have already been performed by Shirley,[15] and later by Elliot.[16] However, due to the paramount difficulties encountered when taking measurements in sediments, there was too much scatter in their data to be able to make any definite conclusion about their results.

After making a few modifications in their technique, new measurements have been taken and have been shown to be repeatable. The main modification has been the redesign of the compressional wave transducer. The transducers were designed so that the Rayleigh distance would be relatively short compared to the size of the sediment sample. Thus, spherical spreading was established at the distances at which the measurements were taken. The spreading losses could then be taken into account when analyzing the data so that the attenuation could be determined.

An important by-product of the new design was the wide beam pattern of the new transducer, which was fairly wide. As a result, the sound pressure level is essentially constant for small angles off the axis of the transducer. This enables the transducer to be repositioned at a new separation without the amplitude being affected by the directivity of the transducer. Thus, we were confident that the decay in amplitude was caused only by increasing the separation of the transducers.

At this point, having confidence in the measurement techniques, the phase velocity and attenuation as functions of viscosity can be determined. These measurements, once taken, can then be compared to the predictions of the Biot-Stoll theory.

ACKNOWLEDGMENTS

In the process of writing this report, we were fortunate to receive contributions and support from several persons. Dr. Ilene Busch-Vishniac answered many questions, particularly those involving the design of the transducers and error analysis. The transducer design was primarily the result of two conversations with Dr. Elmer Hixson. Mr. Ken Kirksey also made several contributions in the development of the transducers, particularly in their construction. We were fortunate to have had the opportunity to visit Dr. James Matthews's lab at NORDA in Bay St. Louis, Mississippi, and to witness some of the progress he has made in experimental sediment acoustics. We are also indebted to Mr. Donald J. Shirley and Mr. Kenneth P. Elliot for their previous work in the sediments laboratory at ARL:UT; to Ms. Jo Lindberg, who also worked on this project; and to Mr. James TenCate, who made several contributions in the instrumentation.

REFERENCES

1. D. J. Shirley and A. L. Anderson, "Studies of Sediment Shear Waves, Acoustical Impedance, and Engineering Properties", Applied Research Laboratories Technical Report No. 75-23 (ARL-TR-75-23), Applied Research Laboratories, The University of Texas at Austin, 7 May 1975.

2. D. J. Shirley and A. L. Anderson, "In Situ Measurement of Marine Sediment Acoustical Properties during Coring in Deep Water", IEEE Trans. Geosci. Electronics 13, (4) (1975).

3. D. J. Shirley and L. D. Hampton, "Shear Wave Measurements in Laboratory Sediments", J. Acoust. Soc. Am. 63, 607 (1978).

4. J. M. Hovem and G. D. Ingram, "Viscous Attenuation of Sound in Saturated Sand", J. Acoust. Soc. Am. 66, 1807-1811 (1979).

5. M. O'Donnell, E. T. Jaynes, and J. G. Miller, "Kramers-Kronig Relationship between Ultrasonic Attenuation and Phase Velocity", J. Acoust. Soc. Am. 69 (3), 696-701 (1981).

6. F. B. Jensen and W. A. Kuperman, "Optimum Frequency of Propagation in Shallow Water Environments", J. Acoust. Soc. Am. 73, 813-819 (1983).

7. E. L. Hamilton, "Geoacoustic Modeling of the Sea Floor", J. Acoust. Soc. Am. 68, 1313-1340 (1980).

8. R. D. Stoll and G. M. Bryan, "Wave Attenuation in Saturated Sediments", J. Acoust. Soc. Am. 47, 1440-1447 (1970).

9. R. D. Stoll, "Acoustic Waves in Saturated Sediments", in Physics of Sound in Marine Sediments, L. D. Hampton, ed. (Plenum Press, New York, 1974), pp. 19-39.

10. R. D. Stoll, "Acoustic Waves in Ocean Sediments", Geophysics 42, 715-725 (1977).

11. R. D. Stoll, "Theoretical Aspects of Sound Transmissions in Sediments", J. Acoust. Soc. Am. 68, 1341-1349 (1980).

12. M. A. Biot, "Theory of Propagation of Elastic Waves in a Fluid-Saturated Porous Solid, I. Low-Frequency Range", J. Acoust. Soc. Am. 28, 168-178 (1956).

13. M. A. Biot, "Theory of Propagation of Elastic Waves in a Fluid-Saturated Porous Solid, II. Higher Frequency Range", J. Acoust. Soc. Am. 28, 179-191 (1956).

14. A. Bedford, D. Costley, and M. Stern, "On the Drag and Virtual Mass Coefficients in Biot's Equations", J. Acoust. Soc. Am. 76, 1804-1809 (1984).

15. D. J. Shirley, "Acoustical Properties of Sediments", Applied Research Laboratories Technical Report No. 81-20 (ARL-TR-81-20), Applied Research Laboratories, The University of Texas at Austin, 11 May 1981.

16. A. Bedford, G. Ellis, K. P. Elliot, S. K. Mitchell, and D. J. Shirley, "Acoustical Properties of Sediments", Applied Research Laboratories Technical Report No. 82-47 (ARL-TR-82-47), Applied Research Laboratories, The University of Texas at Austin, 2 September 1982.

17. David W. Bell, "Shear Wave Propagation in Unconsolidated Fluid Saturated Porous Media", Applied Research Laboratories Technical Report No. 79-31 (ARL-TR-79-31), Applied Research Laboratories, The University of Texas at Austin, 15 May 1979.

18. David T. Blackstock, Notes for ME/EE 384N.1 and 384N.2, "Acoustics I and II", courses given in Departments of Mechanical Engineering and Electrical Engineering at The University of Texas at Austin, 1983-84.

19. Madison L. Sheely, Industrial and Engineering Chemistry 24, 1060-1064 (1932).

20. Philip R. Bevington, Data Reduction and Error Analysis for the Physical Sciences (McGraw-Hill Book Co., Inc., New York, 1969).

8 May 1985

DISTRIBUTION LIST FOR
ARL-TR-85-13
UNDER CONTRACT N00014-83-K-0696

Copy No.

Director
Office of Naval Research Detachment, Bay St. Louis
NSTL, MS 39529
1 Attn: G. Morris (Code 425GG)
2 D. Epp (Code 425GG)

Chief of Naval Research
Department of the Navy
Arlington, VA 22217
3 Attn: Chief of Naval Research
4 R. F. Obrochta (Code 425AR)
5 M. McKisic (Code 4250A)
6 R. Fitzgerald (Code 425UA)
7 J. Heacock (Code 425GG)
8 J. Kravitz (Code 425GG)

Commanding Officer
Naval Ocean Research and Development Activity
NSTL Station, MS 39529
9 Attn: E. D. Chaika (Code 270)
10 R. Gardner (Code 201)
11 D. Lavoie (Code 363)
12 R. Martin (Code 110A)
13 J. Matthews (Code 362)
14 K. Gilbert (Code 362)
15 A. Eller (Code 115)
16 W. Carey (Code 113)

Commanding Officer
Space and Naval Warfare Systems Command
Department of the Navy
Washington, DC 20360
17 Attn: LT B. Ogg (Code 612)

Director
Naval Research Laboratory
Department of the Navy
Washington, DC 20375
18 Attn: R. Dicus (Code 5128)
19 R. Gragg (Code 5160)

Dist. list for ARL-TR-85-13 under Contract N00014-83-K-0696 (cont'd)

Copy No.

Commanding Officer
Naval Ocean Systems Center
San Diego, CA 92152
20 Attn: H. P. Bucker
21 R. Bachman (Code 541)

Chief of Naval Operations
Department of the Navy
Washington, DC 20350
22 Attn: CDR C. Spikes (OP 952D)

23 Commander
Naval Surface Weapons Center
White Oak Laboratory
Silver Spring, MD 20910

24 Commander
David W. Taylor Naval Ship Research and
Development Center
Bethesda, MD 20034

Commanding Officer
Naval Oceanographic Office
NSTL, MS 39522
25 Attn: W. Jobst (Code 7300)

Commander
Naval Air Development Center
Warminster, PA 18974
26 Attn: C. L. Bartberger

Commander
New London Laboratory
Naval Underwater Systems Center
New London, CT 06320
27 Attn: P. Herstein
28 H. Weinberg

Superintendent
Naval Postgraduate School
Monterey, CA 93943
29 Attn: Library

Commander
Naval Coastal Systems Center
Panama City, FL 32407
30 Attn: G. McLeroy

Dist. list for ARL-TR-85-13 under Contract N00014-83-K-0696 (cont'd)

Copy No.

31 - 41	Commanding Officer and Director Defense Technical Information Center Cameron Station, Building 5 5010 Duke Street Alexandria, VA 22314
	Woods Hole Oceanographic Institution 86-95 Water Street Woods Hole, MA 02543
42	Attn: R. Spindel
43	J. Lynch
44	G. Frisk
	Science Applications, Inc. 1710 Goodridge Drive McLean, VA 22101
45	Attn: C. Spofford
46	J. Hanna
	Applied Research Laboratory The Pennsylvania State University P. O. Box 30 State College, PA 16801
47	Attn: S. McDaniel
	Marine Physical Laboratory of The Scripps Institution of Oceanography The University of California, San Diego San Diego, CA 92132
48	Attn: F. Fisher
49	G. Shor
	Scripps Institution of Oceanography The University of California, San Diego La Jolla, CA 92037
50	Attn: Library
	Graduate School of Oceanography University of Rhode Island Kingston, RI 02881
51	Attn: R. Tyce
	Bell Telephone Laboratories, Inc. Whippany Road Whippany, NJ 07961
52	Attn: A. Carter
53	R. Holford

Dist. list for ARL-TR-85-13 under Contract N00014-83-K-0696 (cont'd)

Copy No.

Planning Systems, Inc.
7900 Westpark Drive, Suite 507
McLean, VA 22101
54 Attn: B. Brunson

Defence Scientific Establishment
HMNZ Dockyard
Devonport, Auckland
NEW ZEALAND
55 Attn: K. M. Guthrie

School of Mechanical Engineering
Georgia Institute of Technology
Atlanta, GA 30332
56 Attn: A. D. Pierce
57 P. Rogers

Department of Geology and Geophysics
Geophysical and Polar Research Center
Lewis G. Weeks Hall for Geological Sciences
The University of Wisconsin, Madison
1215 W. Dayton Street
Madison, WI 53706
58 Attn: C. S. Clay

Courant Institute
251 Mercer Street
New York, NY 10012
59 Attn: D. C. Stickler

Hawaii Institute of Geophysics
The University of Hawaii
2525 Correa Road
Honolulu, HI 96822
60 Attn: L. N. Frazer

Director
North Atlantic Treaty Organization
SACLANT ASW Research Centre
APO New York 09019
61 Attn: T. Akal
62 F. Jensen

Defence Research Establishment Pacific
FMO Victoria, BC
VOS 1BO CANADA
63 Attn: R. Chapman
64 J. M. Ozard

Dist. list for ARL-TR-85-13 under Contract N00014-83-K-0696 (cont'd)

Copy No.

Defence Research Establishment Atlantic
9 Grove Street
P. O. Box 1012
Dartmouth, NS
CANADA
65 Attn: D. Chapman

The Catholic University of America
6220 Michigan Avenue, NE
Washington, DC 20017
66 Attn: H. M. Uberall

Lamont-Doherty Geological Observatory
Columbia University
Palisades, NY 10964
67 Attn: G. Bryan
68 R. D. Stoll

Department of Civil and Ocean Engineering
The University of Rhode Island
Kingston, RI 02881
69 Attn: A. J. Silva

University College of North Wales
Marine Science Laboratories
Menai Bridge
Anglesey, LL59 5EY, U.K.
70 Attn: D. Taylor Smith

Institute of Oceanographic Sciences
Godalming
Surrey GU8 5UB, U.K.
71 Attn: P. Schultheiss

Department of Civil Engineering
The University of Texas at Austin
Austin, TX 78712
72 Attn. K. Stokoe

Southwest Research Institute
P. O. Drawer 28510
San Antonio, TX 78284
73 Attn: D. J. Shirley

Rosenteil School of Marine and
Atomospheric Science
The University of Miami
10 Rickenbacker Causeway
Miami, FL 33149
74 Attn: H. DeFarrari

Copy No.

Applied Physics Laboratory
The Johns Hopkins University
Johns Hopkins Road
Laurel, MD 20810
75 Attn: J. Lombardo
76 R. Henrick
77 A. Boyles

Department of Ocean Engineering
Massachusetts Institute of Technology
Cambridge, MA 02139
78 Attn: I. Dyer
79 G. Duckworth
80 A. Baggeroer

The University of Miami
10 Rickenbacker Causeway
Miami, FL 33149
81 Attn: F. Tappert

Department of Physics
The University of Rhode Island
Kingston, RI 02881
82 Attn: C. Kaufman

Department of Electrical Engineering
Polytechnic Institute of New York
Farmingdale, NY 11735
83 Attn: L. B. Felsen

84 I. Tolstoy
Knockvennie, Castle Douglas
S. W. SCOTLAND
GREAT BRITAIN

Department of Geology
The University of Texas at Austin
Austin, TX 78712
85 Attn: C. Wilson
86 M. Backus

Department of Electrical Engineering
The University of Texas at Austin
Austin, TX 78712
87 Attn: E. Hixson

Department of Physics
The University of Auckland
Private Bag, Auckland
NEW ZEALAND
88 Attn: A. C. Kibblewhite
89 C. T. Tindle

Dist. list for ARL-TR-85-13 under Contract N00014-83-K-0696 (cont'd)

Copy No.

	Chinhae Research Laboratory P. O. Box 18 Chinhae, Kyeong Nam KOREA
90	Attn: Jungyul Na
	Department of Oceanography Texas A&M University College Station, TX 77843
91	Attn: A. Anderson
	Department of Geological Oceanography Texas A&M University College Station, TX 77843
92	Attn: W. Bryant
	Sandia National Laboratories Division 7552 Albuquerque, NM 87185
93	Attn: W. Shurteleff
94-95	D. Costley
96	A. Marc Bedford, ARL:UT
97	H. Boehme, ARL:UT
98	Robert A. Koch, ARL:UT
99	Stephen K. Mitchell, ARL:UT
100	T. G. Muir, ARL:UT
101	Clark S. Penrod, ARL:UT
102	Morris Stern, ARL:UT
103	Paul J. Vidmar, ARL:UT
104	Gary R. Wilson, ARL:UT
105	Ching H. Yew, ARL:UT
106	Library, ARL:UT

END

FILMED

12-85

DTIC